Zeitschrift: Eclogae Geologicae Helvetiae

Herausgeber: Schweizerische Geologische Gesellschaft

Band: 73 (1980)

Heft: 2: Symposium alpine geotraverses with special emphasis on the Basel-Chiasso profile : Lausanne, 4-5 October 1979

Artikel: A model of the Jorat magnetic anomaly based on the three field components

Autor: Fischer, Gaston / Le Quang, Bac Viet

DOI: https://doi.org/10.5169/seals-164984

Eclogae geol. Helv.	Vol. 73/2	Pages 663-679	10 figures in the text and 2 tables	Basle, July 1980

A model of the Jorat magnetic anomaly based on the three field components

By GASTON FISCHER and BAC VIET LE QUANG[1])

ABSTRACT

The new survey of the geomagnetic field in Switzerland has confirmed the highly symmetrical character of the Jorat anomaly and suggested an interpretation based on the three vector components of the field. To this end, analytic formulae have been set up, which give the field produced by a prism in the shape of a rectangular parallelepiped, uniformly magnetized in an arbitrary direction. Through translations and rotations it is possible to position this prism at will beneath the plane of the observed anomaly. The field produced by the prism is then compared with the field that was actually measured and the prism parameters are systematically varied in order to minimize the mean square difference of the two fields over the various observation sites. For the Jorat anomaly 39 sites within a 60×60 km square have been used. The best prism found is fairly similar to the one proposed by MEYER DE STADELHOFEN et al. (1973) but it shows a definite dip to the south and is buried at greater depth. At this depth the prism is inside the hercynian basement, of which it probably reflects the regional structure. This would confirm that the causative body of the Jorat anomaly was formed before the Alps.

RÉSUMÉ

Le nouveau levé géomagnétique de la Suisse a confirmé le caractère hautement symétrique de l'anomalie du Jorat et nous a incités à tenter une interprétation qui tienne compte de toutes les composantes du vecteur magnétique. A cet effet nous avons établi les formules analytiques qui décrivent le champ produit par un prisme en forme de parallélépipède rectangle, magnétisé uniformément dans une direction quelconque. Par le biais de translations et rotations, il est possible d'amener ce prisme dans une position quelconque au-dessous de l'anomalie étudiée. On compare alors le champ produit par le prisme avec le champ effectivement mesuré et on modifie systématiquement les divers paramètres du modèle de façon à minimaliser l'écart quadratique moyen sur l'ensemble des divers points de mesure. Dans le cas de l'anomalie du Jorat, nous disposons de 39 points de mesure répartis sur un carré de 60 km de côté. Le meilleur prisme trouvé est assez semblable à celui proposé par MEYER DE STADELHOFEN et al. (1973) mais est enfoui plus profondément et accuse un pendage marqué vers le sud. A la profondeur proposée ce prisme est situé dans le socle hercynien, dont il pourrait être un reflet de la structure régionale. Son origine serait donc antérieure à celle de la formation des Alpes.

1. Introduction

The Jorat geomagnetic anomaly has become a well-known feature of the geomagnetic maps of Switzerland ever since BRÜCKMANN (1930, 1931) completed his survey. The most striking characteristics of the Jorat anomaly can be summarized as follows: 1. It is well isolated from any of the nearby Alpine anomalies, suggest-

[1]) Observatoire cantonal, CH-2000 Neuchâtel (Suisse).

ing that its origin is not connected with the formation of the Alps. 2. It is highly symmetrical, indicating that its causative body is probably of very simple geometry. 3. It is reasonably large in extent (50×50 km or more) and very smooth, i.e. free of such short wavelength disturbances as characterize the geomagnetic field in the area of the Ivrea body, thus pointing to a singly connected formation at appreciable depth. These rather ideal characteristics have certainly played a role in motivating modelling attempts. Around 1945 MERCANTON & WANNER (1943, 1946) interpreted a N26°W profile of the vertical and horizontal components, respectively Z and H, in terms of a horizontal right prism of somewhat irregular cross-section, suggesting a slight subvertical dip toward the south (cf. Table 1). Then MEYER DE STADELHOFEN et al. (1973) carried out an extensive total field survey and interpreted their data in terms of an almost vertical rectangular prism at a depth to the ceiling of 4.3 ± 0.4 km, dipping at $90 \pm 10°$, and whose principal axis is oriented in a N66°E direction, i.e. almost at a right angle to the MERCANTON & WANNER (1946) profile (cf. Table 1).

A new survey of the geomagnetic field vector having recently been carried out in Switzerland (FISCHER & SCHNEGG 1977; FISCHER et al. 1979), it was tempting to ask if an interpretation based on the three Cartesian components (X, Y, Z) of the field vector F would allow more definite pronouncements as to the depth to the causative body, its dipping angle ($\Pi/2 - \vartheta$ in Fig. 1), and whether its magnetization

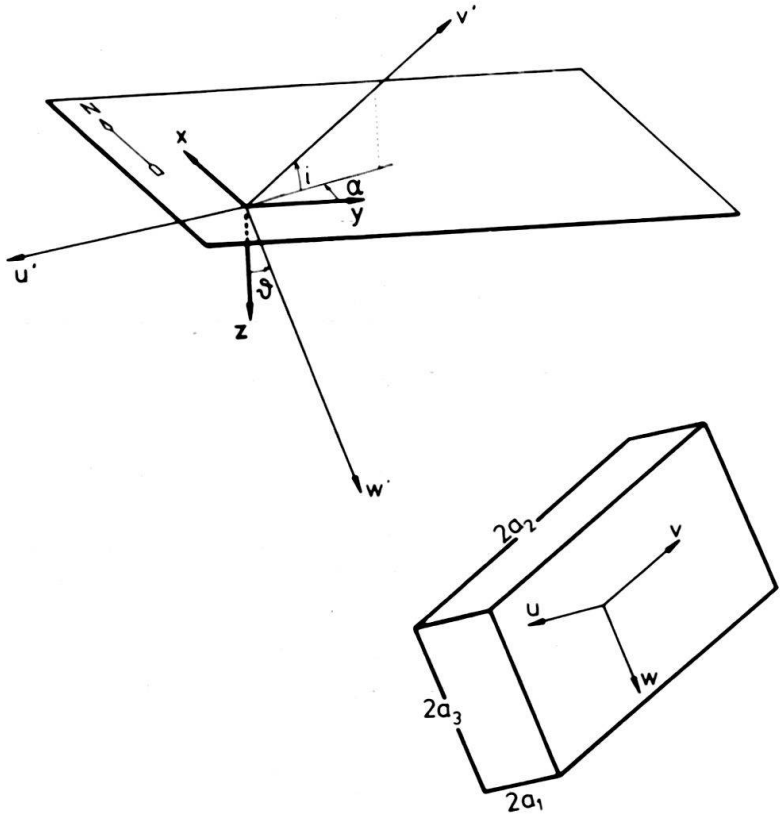

Fig. 1. Respective positions of the geographic coordinate system (x, y, z), with the plane $z=0$ containing the observations sites, and the coordinate system (u, v, w) along the axes of symmetry of the rotated prism. The translated system (u', v', w') serves to illustrate the rotations of (u, v, w) with respect to (x, y, z).

is entirely induced or is largely remanent. Because of the high symmetry of the Jorat anomaly, it was postulated that modelling in terms of a rectangular prism of arbitrary position, orientation, dimensions and magnetization would prove to be very suitable. To reduce the initial computational effort, modelling with the arbitrary rectangular prism was first carried out only for induced magnetization, thus reducing the three free magnetization parameters to a single one of susceptibility. But evidence will be presented indicating that there could be as much as 30% magnetization at right angles to the normal or primary field. With one parameter for susceptibility, three each for position, orientation and dimensions, we are still left with the rather big task of adjusting ten free variables in view of obtaining a best fit.

In our scheme we calculate the field produced in three-dimensional space by a rectangular prism oriented along the axis of a Cartesian coordinate system (u, v, w), as shown in Figure 1. This system is then moved and rotated with respect to the fixed (x, y, z) geographic system, in the $z=0$ plane of which the field has been measured at a certain number of observation sites. For x and y we choose the Swiss military kilometric coordinates (cf. FISCHER et al. 1979). The rotation in space is expressed in terms of the angles a, i and ϑ, where $\Pi/2-a$ is the azimuth with respect to north of the horizontal projection of the principal prism axis, i is the inclination of this axis, and $\Pi/2-\vartheta$ is the dip angle. To insure unequivocality of these angles we request $-\Pi/2<a<\Pi/2$, $-\Pi/2<i<\Pi/2$ and $0<\vartheta<\Pi/2$. Let B_{cj} be the calculated field components for a given set of adjustable or free parameters. The index j runs from 1 to $3n$, n being the number of observation sites. Similarly we label B_{0j} the corresponding observed or measured field components and calculate the standard or mean-square deviation σ between the observed and calculated field:

$$\sigma=\left[\frac{1}{3n}\sum_{j=1}^{3n}(B_{0j}-B_{cj})^2\right]^{1/2} \tag{1}$$

The free parameters are then systematically varied so as to make σ smaller and smaller. The set of parameters yielding the smallest possible σ then corresponds to the best possible rectangular prismatic model of the body causing the anomaly.

2. The field of a uniformly magnetized rectangular prism

In this section the magnetic field produced by a uniformly magnetized rectangular prism is calculated under the assumption that demagnetizing effects can be neglected. For the weak fields and low susceptibilities considered here this assumption is perfectly justified. The simplest way of deriving the field produced by the magnetized prism is via the magnetic scalar potential A (e.g. CORSON & LORRAIN 1962),

$$A=\frac{\mu_0}{4\Pi}\int_V\left[\mathbf{M}\cdot\nabla\frac{1}{|\mathbf{r}-\mathbf{r}_0|}\right]d^3\mathbf{r}_0, \tag{2}$$

such that the calculated field is then given by

$$\mathbf{B}_c=-\nabla A=-\left(\frac{\partial A}{\partial x},\ \frac{\partial A}{\partial y},\ \frac{\partial A}{\partial z}\right). \tag{3}$$

Integration in equation (2) is over the volume V of the prism, $\mathbf{r}_0$ thus describing a point inside the prism, whereas $\mathbf{r}$ is the field point, i.e. in general a point outside the prism, where the field is to be calculated. When the magnetization is constant, equation (2) can be transformed to a surface integral,

$$A = \frac{\mu_0 \mathbf{M}}{4\Pi} \int_S \frac{\mathbf{ds}}{r}, \tag{4}$$

where $r = |\mathbf{r} - \mathbf{r}_0|$ and $\mathbf{ds}$ is a vectorial element of prism surface.

As was said in section 1, the field will be computed for a rectangular prism whose axes are parallel to the coordinate axes (u, v, w) of Figure 1. For the ease of notation, however, we switch temporarily to the coordinate system (and notation) represented in Figure 2. Introducing $\mathbf{m} = \mu_0 \mathbf{M}/4\Pi$ we can write

$$A = \sum m_j (I_{j+} - I_{j-}), \qquad j = 1,2,3, \tag{5}$$

where

$$I_{j\pm} = \int_{S_{j\pm}} \frac{ds}{r}, \tag{6}$$

$S_{j\pm}$ referring to the six faces of the prism, as depicted in Figure 2.

To obtain the field B_c it is necessary, according to equation (3), to calculate the derivatives of $I_{j\pm}$. There is advantage in taking the derivatives before carrying out the integrations required in equation (6); these integrations then become quite straightforward and lead to the following final result:

$$B_{cj} = \sum m_k (J_{kj+} - J_{kj-}), \tag{7}$$

where j, k, l is a cyclic permutation of the indices 1, 2, 3, with

$$J_{kj+} = \ln \left[\frac{x_l - a_l + r_{j+k-l+}}{x_l - a_l + r_{j+k+l+}} \cdot \frac{x_l + a_l + r_{j+k+l-}}{x_l + a_l + r_{j+k-l-}} \right] \tag{8}$$

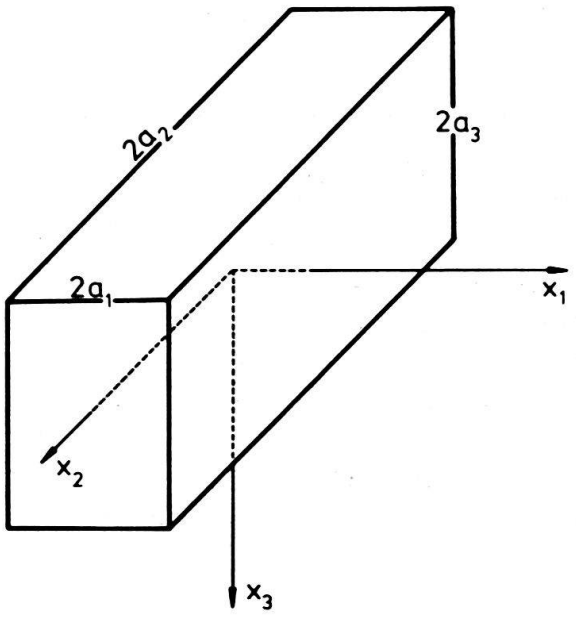

Fig. 2. Coordinate system and notation used in deriving the field produced by a uniformly magnetized prism.

when $k \neq j$, whereas

$$J_{jj+} = \arctan \frac{(x_k - a_k)(x_l - a_l)}{(x_j - a_j) r_{j+k+l+}} - \arctan \frac{(x_k + a_k)(x_l - a_l)}{(x_j - a_j) r_{j+k-l+}}$$

$$- \arctan \frac{(x_k - a_k)(x_l + a_l)}{(x_j - a_j) r_{j+k+l-}} + \arctan \frac{(x_k + a_k)(x_l + a_l)}{(x_j - a_j) r_{j+k-l-}}. \quad (9)$$

In these equations we have introduced the quantities $r_{j\pm k\pm l\pm}$, the definition of which is as follows:

$$r_{j\pm k\pm l\pm} = \sqrt{(x_j \mp a_j)^2 + (x_k \mp a_k)^2 + (x_l \mp a_l)^2}\,. \quad (10)$$

The $r_{j\pm k\pm l\pm}$ thus correspond to the distances between the field point and the eight corners of the prism.

Equations (7) to (10) in effect constitute a recipe for calculating the field B_c generated by the magnetized prism of Figure 2, anywhere in space, and in particular in any specified plane. Translations and rotations, as indicated in Figure 1, can then bring that plane into coincidence with the plane containing the measurement sites of the observed field B_0, i.e. the $z = 0$ plane of Figure 1. This recipe was integrated into an iterative systematic search procedure based on the simplex and on the variable metric methods (JAMES 1972; JAMES & ROOS 1975), for the adjustable parameters which minimize the mean square deviation σ defined in equation (1). Twelve free parameters were available, but to limit computing time this number was initially reduced to ten with the assumption that the magnetization was entirely of induced character, and therefore expressible with a single scalar susceptibility χ only. Once the best model was found (model I of Table 1), it was used as initial condition in the search for an improved model with arbitrary magnetization. In this process the standard deviation could be reduced further, but only by about 10%, as shown in Table 1. Most other model parameters underwent similar small changes, but the overall prismatic model remained the same. For example, it is most likely that there is some remanent magnetization, especially because the primary field is subject to secular variations, but the dominant contribution nevertheless comes from a magnetization parallel to the present normal field, even though it can not be stated what percentage of this magnetization is remanent and what percentage is induced.

3. Comparison with other modelling methods

A rather large number of geomagnetic modelling schemes similar to ours have been proposed by others. To facilitate a brief comparison with some of these other schemes we recall the main characteristics of ours: 1. It tries to model the anomaly with a best-fitting rectangular prism. 2. It searches the most appropriate location, orientation, dimensions, and magnetization of this prism. 3. It takes all the field components into account. Several other schemes set out with more complex model shapes, but probably because of the rapidly growing computational effort required as the number of adjustable parameters increases, these schemes are generally not

implemented in full. For example, HJELT (1972) deals with right prisms of which the section is a parallelogram, so-called dipping prisms with level tops, whereas BARNETT (1976) considers arbitrarily shaped polyhedrons composed of triangular facets, but these two authors do not integrate their calculation into a search scheme to model a given observed anomaly. BHATTACHARYYA (1964, 1978) looks solely at vertical right prisms and tries to fit total field only. MCGRATH & HOOD (1970, 1973) stack rectangular prismatic plates, but the top edge of these plates is always parallel to the ground and fitting is attempted to total field only. WHITEHILL (1973) models with vertical rectangular prisms and PLOUFF (1976) with vertical polygonal prisms only. BOSUM (1966) starts with horizontal prisms of unspecified section, but ends by fitting profiles only. TALWANI'S (1965) approach of stacking horizontal polygonal prisms seems the most general, but the fit achieved in a specific example is rather disappointing; it might be improved upon with today's more powerful computational means. As this comparison of methods suggests, and our own observations seem to confirm, increasing the number of degrees of liberty, i.e. the number of adjustable parameters, does not necessarily render the fitting process more easy. In general the computational requirements increase faster than the number of free parameters, while at the same time the minimum of σ in the parameter space becomes less and less well-defined; it thus becomes more difficult to draw definite conclusions about the most likely range of any of the parameters, especially those of greatest interest, like the angle of dip or the depth to the top of the structure. In this respect, the technique of transformation into isodepths maps of GERARD & DEBEGLIA (1975) might prove especially appropriate.

4. Modelling the Jorat anomaly

In the recent geomagnetic survey of Switzerland (cf. FISCHER & SCHNEGG 1977 and FISCHER et al. 1979), the elements measured were declination D, inclination I, and amplitude F. These elements were transformed into Cartesian components with respect to geographic north (X), geographic east (Y), and local vertical into the ground (Z). Within a 60 by 60 km square, symmetrically bordering the anomaly, 39 field measurements are available for our modelling attempt. The location of the 39 observation sites is shown in Figure 3. This is a rather small number, when compared with the 848 total field data points of MEYER DE STADELHOFEN et al. (1973), but it should be pointed out that each of the three field components of an observation site constitutes independent information, whereas the single amplitude datum of any point of a dense network is obviously highly correlated with the amplitudes at all the neighbouring points.

The results of the search for the best fit are summarized in Table 1, and the model I prism is sketched in Figure 3 together with the prism found by MEYER DE STADELHOFEN et al. (1973). Clearly all these models are quite similar, and the question may be asked, whether there is any new information that can be deduced from the present calculation. A careful look at Table 1 shows that the new data tend to put the ceiling of the causative body at a somewhat greater depth, and seem quite definite about a dip to south of less than the 90° vertical, as suggested already by

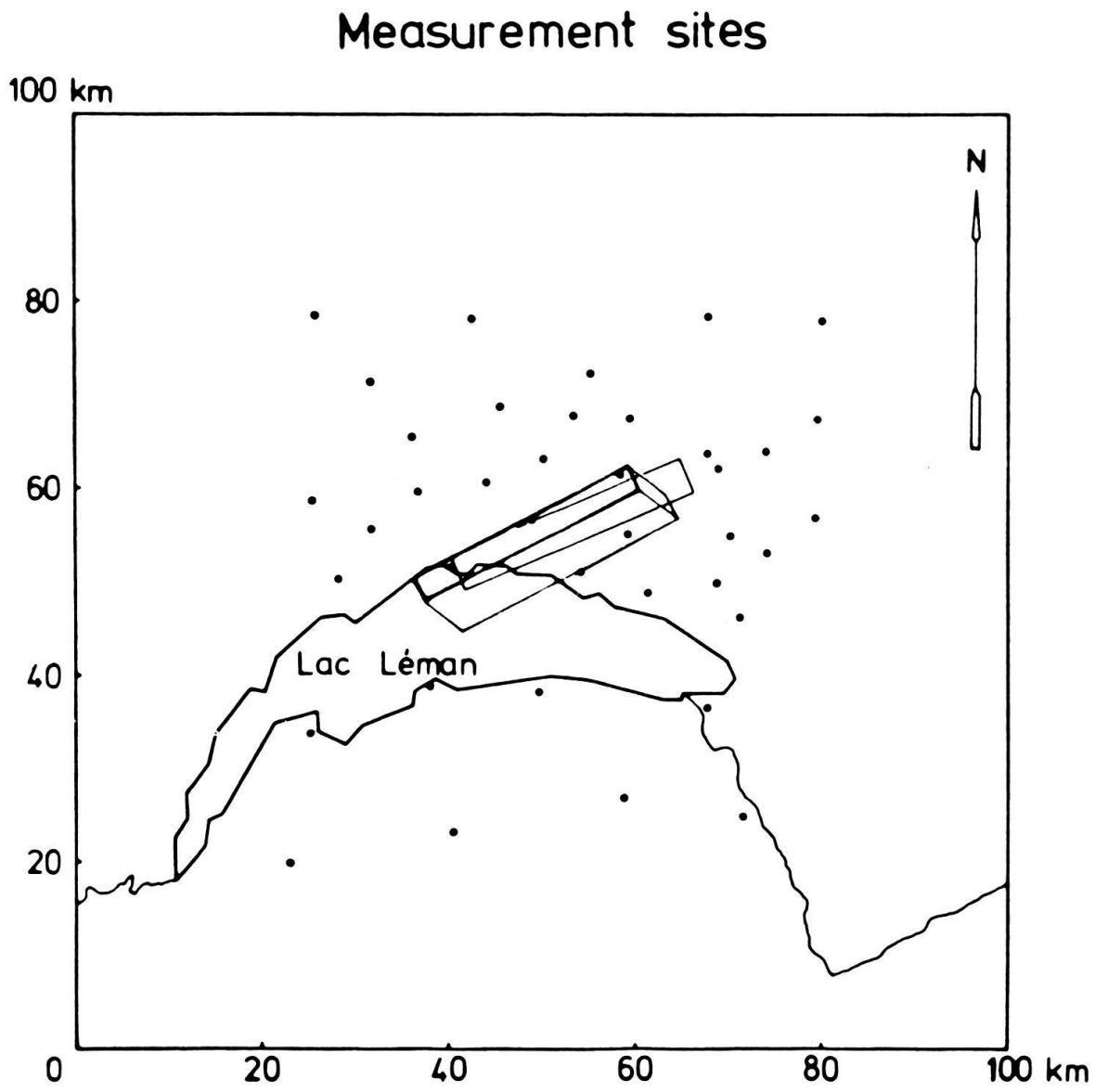

Fig. 3. Situation of the study area around Lake Geneva (Lac Léman), with the measurement sites and sketches of the Model I dipping prism and the MEYER DE STADELHOFEN et al. (1973) vertical prism (cf. Table 1).

MERCANTON & WANNER (1946). Whether or not there is a dip of less than 90°, and whether the depth to the ceiling is of the order of 6 km, rather than 4 km, are probably the two questions of greatest interest to geology. It was therefore decided to investigate these questions further by studying a north-south (N-S) profile, chosen so as to exhibit a very small transverse field component Y. This profile is at kilometric coordinate $y = 542$ km.

Our modelling method is well adapted to two-dimensional studies, i.e. to the study of profiles, especially those profiles without transverse field, for which the plane of the profile simply cuts across the middle of the prism. The search for best fit is much faster here, since the number of free parameters is reduced to 7 (2 for position, 1 for orientation, 2 for dimensions, and 2 for magnetization). The com-

Table 1: *Various models of causative body for the Jorat geomagnetic anomaly.*

Model		I	II	Meyer de Stadelhofen et al.	Mercanton & Wanner
Magnetization		In direction of normal field	Rotated away from normal by about 16° toward NE	In direction of normal field	In direction of normal field
Susceptibility		0.13 SI units	0.49 SI units	0.05 SI units	0.075 SI units
Orientation		N 63.7° E	N 60.6° E	N 66° E	N 64° E
Inclination to W		6.3°	4.9°	$\sim$0°	$\sim$0°
Dip to S($\pi/2-\vartheta$)		74.6°	85.1°	90 $\pm$ 10°	$\sim$80°
Length $2a_2$		26.2 km	24.2 km	$\sim$28 km	
Width $2a_1$		3.3 km	0.8 km	3.6 $\pm$ 0.5 km	3-8 km
Depth to center of upper face		5.6 km	6.0 km	4.3 $\pm$ 0.4 km	
Depth to highest point (e.g. corner)		3.8 km	4.9 km	$\sim$4 km	3.4 km
Assumed depth to bottom face center		25.0 km	25.0 km		20 km
Coordinates of center of upper face	x	154.8 km	155.6 km	$\sim$148.5 km	$\sim$154.6 km
	y	538.3 km	540.2 km	$\sim$ 538.5 km	$\sim$540.4 km
Standard deviation		20.8 nT	18.9 nT		

Table 2: *Modelling on a north-south profile.*

Components fitted		X	Z	X & Z
Amplitude of magnetization		290 nT	320 nT	268 nT
Induced (//) magnetization		289.9 nT	308.2 nT	266.2 nT
Remanent ($\perp$) magnetization		6.6 nT	86.0 nT	31.3 nT
Ratio (remanent/induced)		2.2%	28%	11.7%
Inclination of magnetization		60.9°	46.6°	55.5°
Susceptibility χ		0.079 SI units	0.084 SI units	0.072 SI units
Dip to S($\pi/2-\vartheta$)		63.2°	85.4°	64.2°
Width $2a_1$		4.5 km	7.5 km	6.7 km
Depth to center of top edge		7.4 km	8.3 km	8.0 km
Depth to uppermost corner		6.3 km	8.0 km	6.5 km
Coordinates of center of prism	x	143.4 km	145.9 km	143.9 km
	y	542.0 km	542.0 km	542.0 km
Assumed length of prism $2a_2$		32.0 km	32.0 km	32.0 km
Assumed depth to center of bottom edge		25.0 km	25.0 km	25.0 km
Standard deviation		10.5 nT	4.9 nT	16.0 nT

ponents to be fitted are X or Z, or both simultaneously. The results are shown in Table 2 and Figure 4, and it is seen that whenever the magnetization is almost entirely in the direction of the normal field the best-fitting prism indeed slants away quite markedly toward the south. On the other hand, just as in the three-dimensional modelling (i.e. modelling over the entire $z=0$ plane), when the magnetization vector turns upward the prism seems to rotate into a more nearly vertical orientation. What the two-dimensional study also confirms is that the prism really seems to be in the depth range of 6 to 8 km, rather than around 4 km.

Because the study of profiles does require so much less computer time, we have made a brief study of the topography of the minimum of σ in parameter space, for the case of the simultaneous fitting of X and Z. This shows in Figure 5 that the minimum is rather a broad one. For the susceptibility this is not surprising, since for such deeply buried bodies as our prisms, the susceptibility χ and the prism width $2a_1$ are not separately relevant, only their product. In effect, for both models I and II of Table 1, the susceptibility could as well be $\chi=0.49$ and $2a_1=0.8$ km, rather than, respectively, 0.12 and 3.3 km, practically without affecting any of the other parameters, including the fit indicator σ. For the dip angle $\Pi/2-\vartheta$ and the depth to the top corner, however, it may seem surprising to find that the minimum of σ is so wide. But this appears to be a general characteristic of all the geomagnetic modelling schemes we have studied. Furthermore, mean-square deviations are generally larger than 20 nT, and the values found in the present study can be considered very satisfactory, especially as concerns the three-dimensional modelling. This is also in some measure a consequence of the smoothness of the Jorat anomaly, as mentioned at the beginning.

To give a better idea of the degree of success of our three-dimensional modelling we show, in Figures 6 and 7, two maps of component X. Figure 6 corresponds to the observed field and Figure 7 to the calculated field. Similarly Figure 8 and 9 show the observed and calculated Y components. Clearly, the correspondence is very good indeed.

Before concluding we should like to look at the question of the dip from another point of view. Let us assume a paramagnetic causative regular prism, without remanent magnetization. Suppose first that this prism is slanting in about the same direction as the lines of force of the normal field, i.e. that it is dipping north with an angle of about 65° as sketched in Figure 10*a*. It is easy then to convince oneself that the field pattern produced by such a prism will exhibit deep, narrow, and almost antisymmetric lobes along a N-S profile. For inclination I and vertical component Z the positive lobe is north and for the horizontal component the positive lobe is in the south. But if, as sketched in Figure 10*b*, the same paramagnetic prism is oriented so as to be dipping south with an angle of 60 to 80°, then the lobes, while remaining qualitatively the same, would lose their highly antisymmetric character. The southern lobes would become much wider but very shallow, while the northern lobes would remain strong, but probably become somewhat wider than for a prism dipping north. The observations (see the maps of FISCHER et al. 1979) are in perfect accord with the expectations following from a dip toward the south, as seen in Figure 6 for example. However, as we have seen, it is also possible to explain the observations with an almost vertical prism, if the magnetiza-

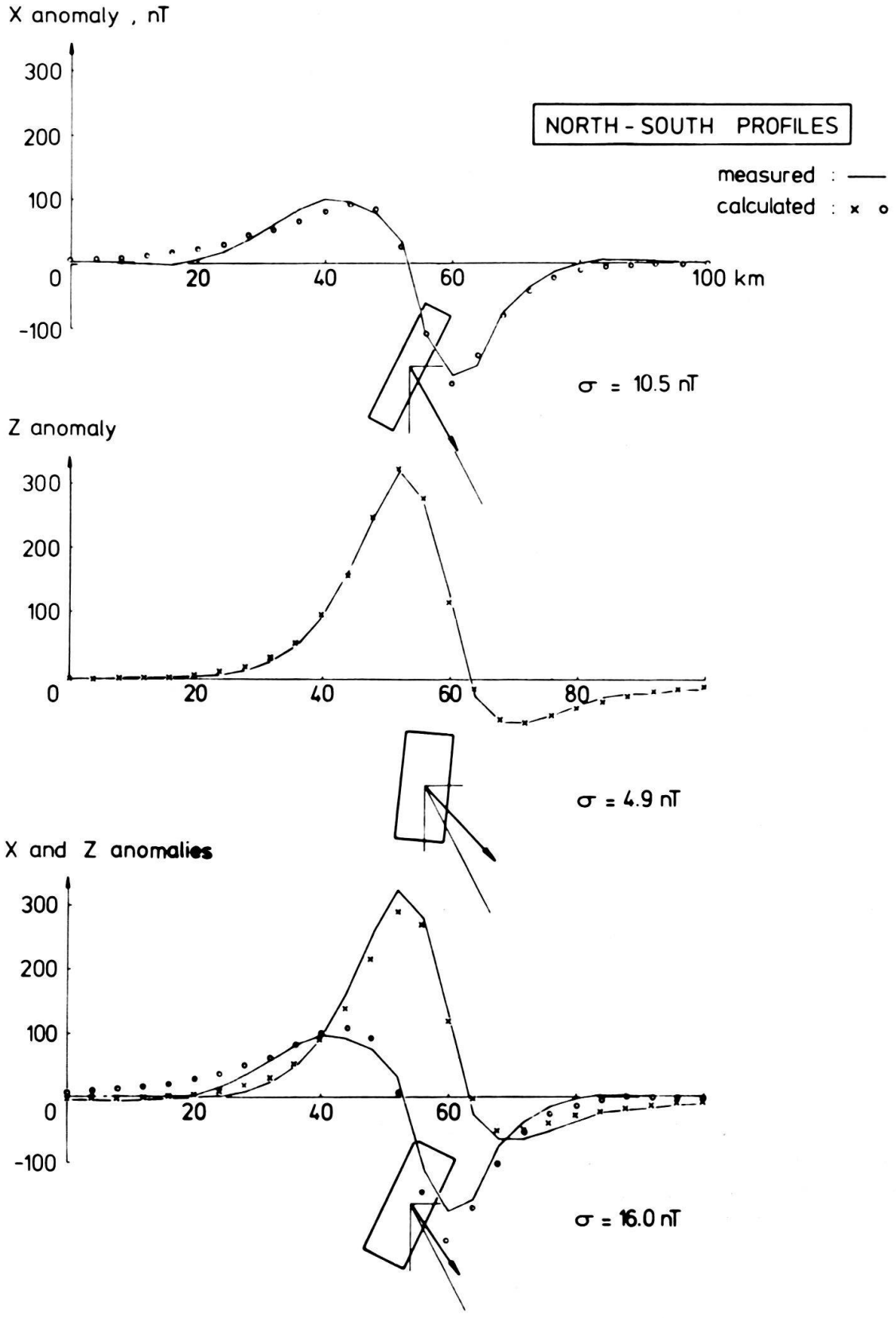

Fig. 4. Results of two-dimensional modelling along a N-S profile at $y = 542$ km. The curves represent the observed data, whereas the dots are calculated (cf. Table 2).

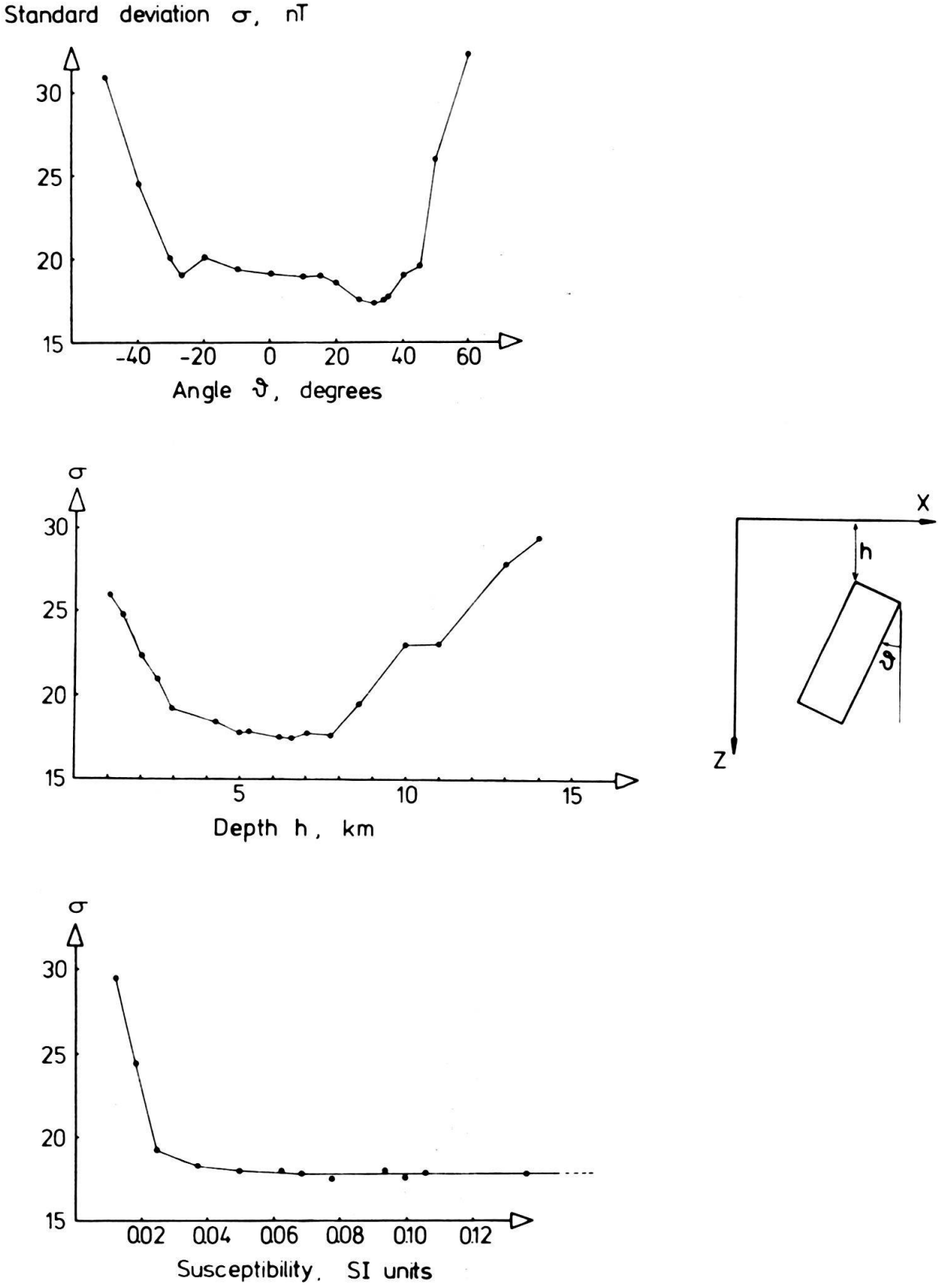

Fig. 5. Topography of the standard deviation minimum in parameter space. Note the independence of σ above a susceptibility of about 0.06 SI units, in which range the product $2a_1\chi$ remains constant. In this diagram ϑ represents ($\Pi/2-$ dip angle), and $\vartheta>0$ means a prism dipping south, $\vartheta<0$ a prism dipping north.

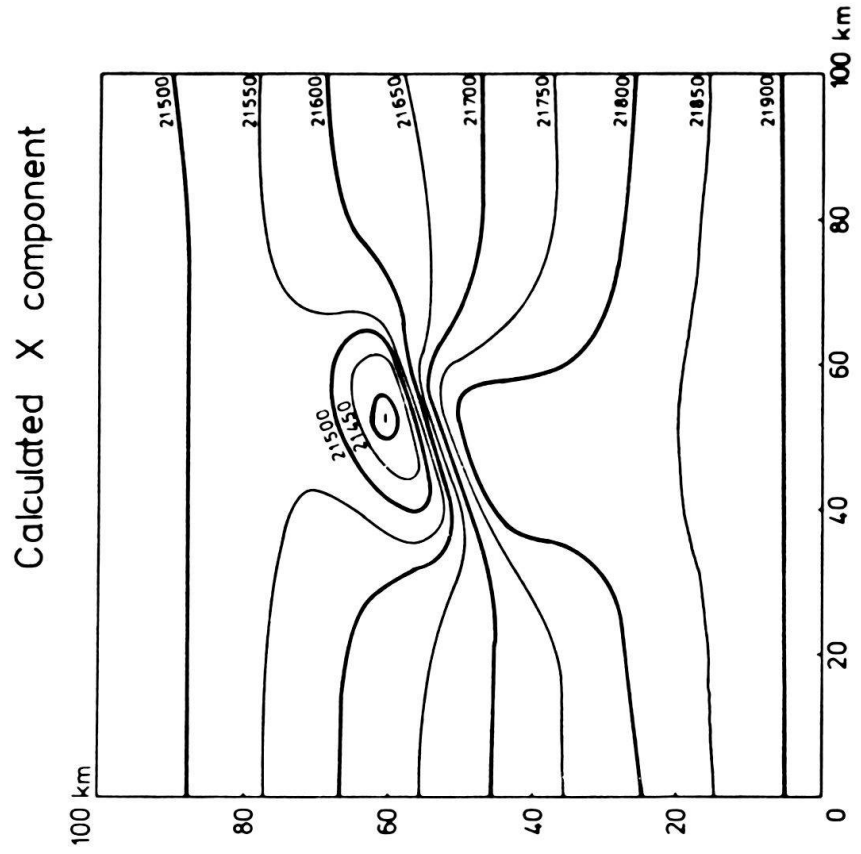

Fig. 7. Calculated X component in the study area.

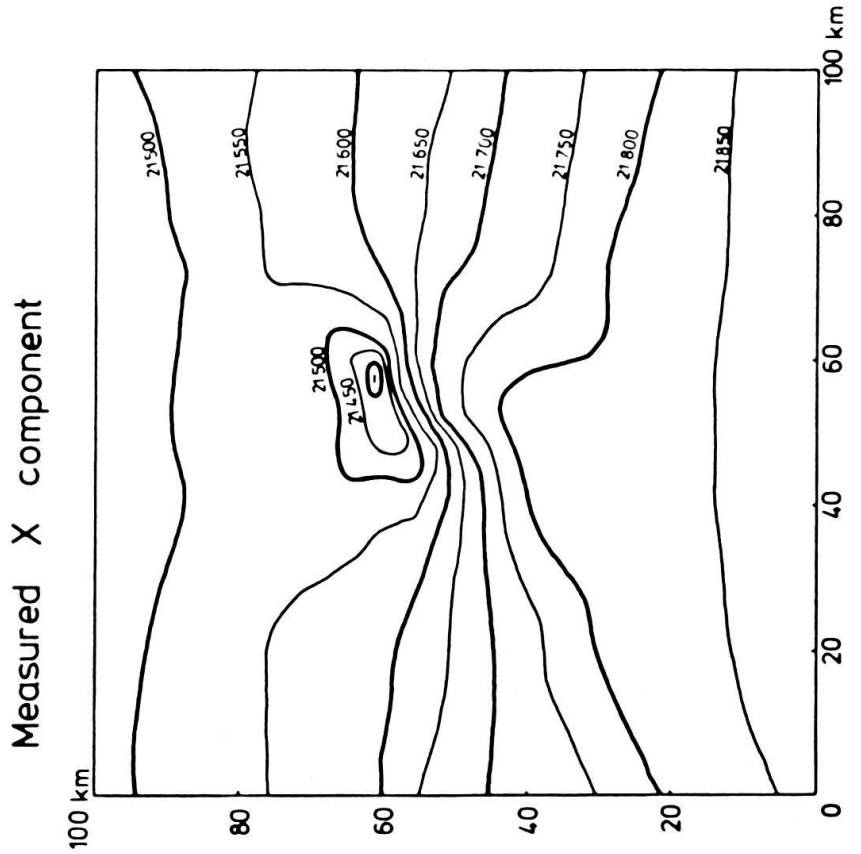

Fig. 6. Measured or observed X component in the study area.

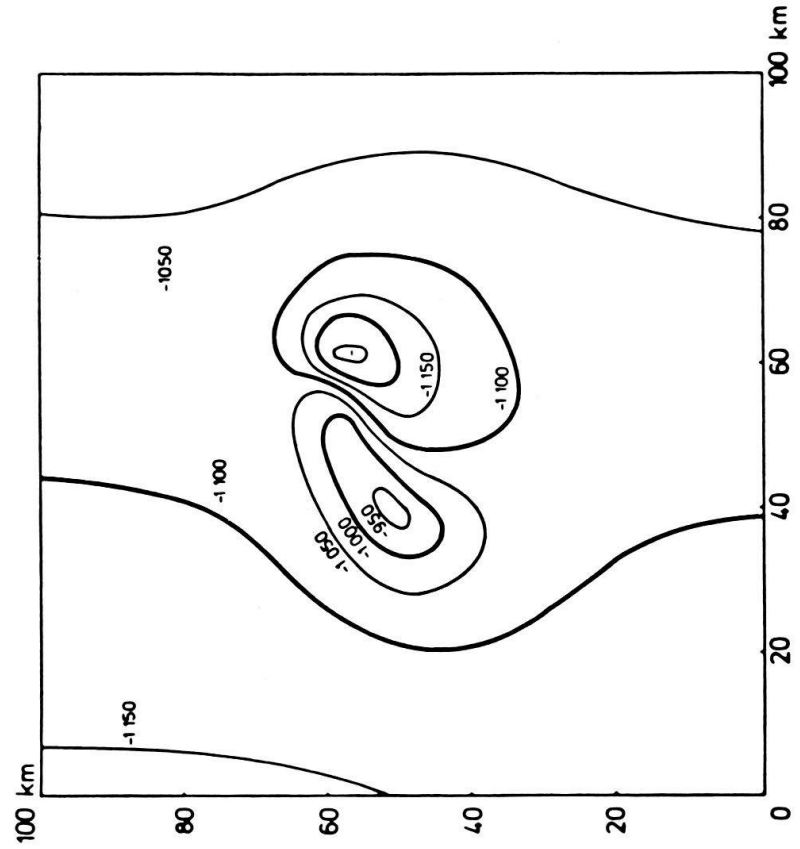

Fig. 9. Calculated Y component in the study area.

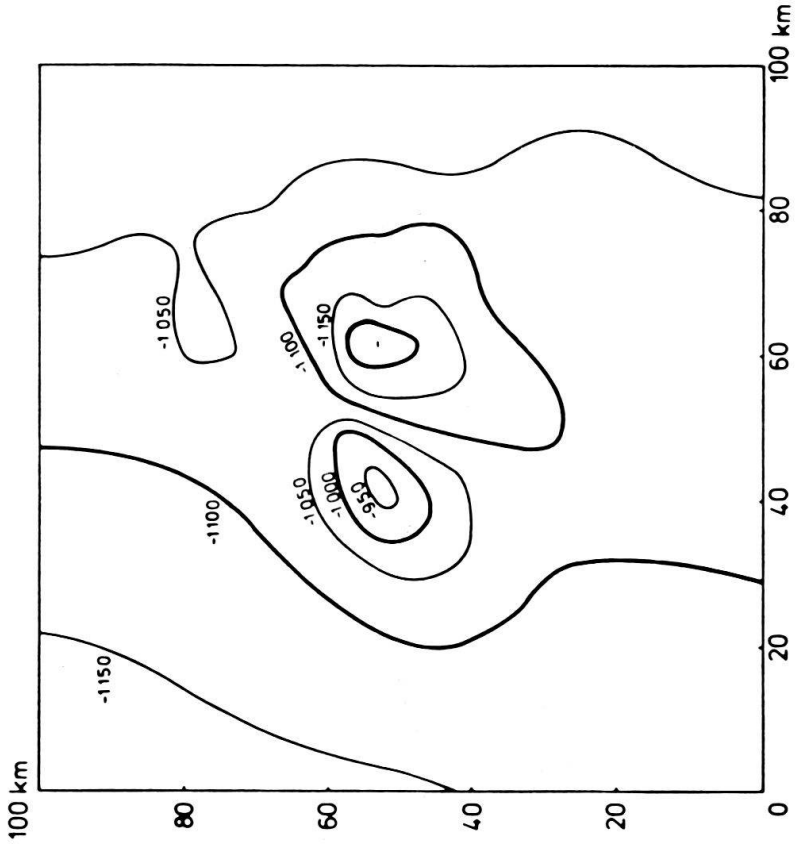

Fig. 8. Measured Y component in the study area.

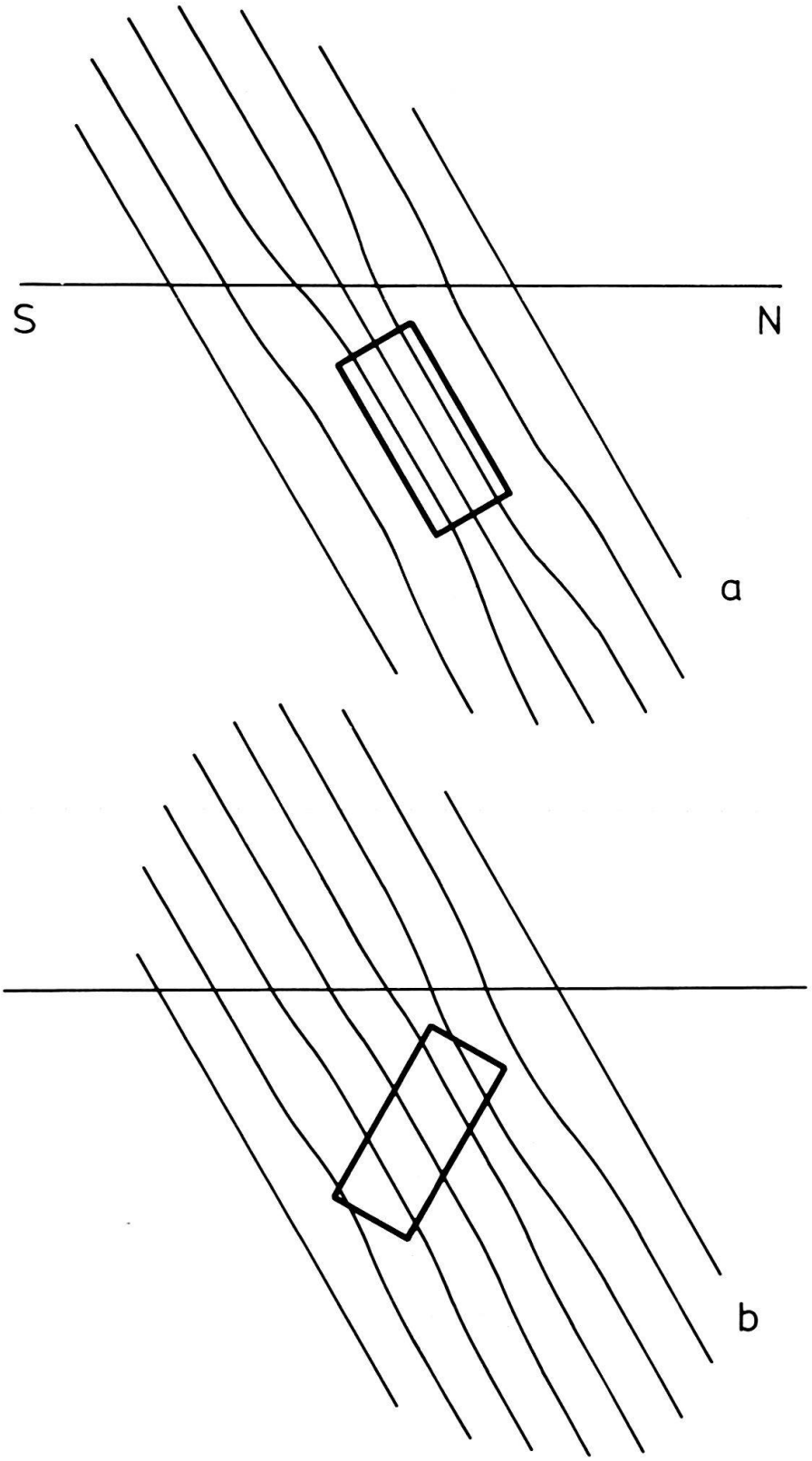

Fig. 10. Sketch to illustrate the anomalies produced by a paramagnetic prism. In *a* the prism is oriented along the field lines and produces strong and concentrated antisymmetric lobes, such that inclination and vertical component are increased in the north and horizontal component in the south. When the prism is dipping south, as in *b*, the northern lobes are similar but perhaps wider than in *a*, but the southern lobes become very shallow, as is observed in Figure 6 for example (see also the maps of FISCHER et al. 1979).

tion is allowed to turn upward, assuming an inclination substantially smaller than that of the normal field.

It may also be asked whether a slanting prism with a level top, which would imply a nonrectangular cross-section (but which may appear more likely from a geological point of view) could not fit the observations better than our regular prisms. So far the answer seems to be negative. Since profiles are easier to tackle than the full three-dimensional problem, we have modelled profiles with prisms whose section is a parallelogram, leaving the angle of the parallelogram free to adjust. The best fit was obtained with nearly rectangular cross-sections close to the results of Figure 4.

5. Conclusions

The present study of the Jorat anomaly seems to suggest that the causative body is a prism of almost constant cross-section, stretching in a N64°E direction and centered at about $x=155$ km, $y=538$ km. The cross-section can be modelled reasonably well with a rectangle dipping away from the vertical toward the south at a dip angle of about $70\pm10°$. The length of the body is about 26 km and is slightly inclined, dropping westward at an angle of close to 6°. The depth to the body is around 4 km at its uppermost northeast corner, but the average depth, i.e. the depth to the center of the upper face, is around 6 km. The width of the body is rather ill-defined, but the product of width time susceptibility is very close to 0.40, so that an apparently reasonable width of 3.3 km also yields a very reasonable susceptibility of 0.12 SI units. Our investigations do not, so far at least, favor a cross-section with nearly level top.

The geological implications of these findings are that the causative body is almost entirely within the hercynian basement; an outcrop into the mesozoic cover is likely at its northeast end only. As far as the origin of this body is concerned it may be looked upon as a dike, associated with a fracture, as proposed by MEYER DE STADELHOFEN et al. (1973), or it may simply reflect the regional hercynian structure in this area. It is probably hazardous, at this time, to push speculations further.

Acknowledgments

This research was supported in part with a grant from the Swiss National Science Foundation. The authors also express their thanks to Professor J.-P. Schaer for geological advice and to Dr. P.-A. Schnegg for computational help.

REFERENCES

BARNETT, C.T. (1976): *Theoretical Modeling of the Magnetic and Gravitational Fields of an Arbitrarily Shaped Three-Dimensional Body.* - Geophysics *41*, 1353-1364.

BHATTACHARYYA, B.K. (1964): *Magnetic Anomalies due to Prism-Shaped Bodies with Arbitrary Polarization.* - Geophysics *29*, 517-531.

— (1978): *Computer Modeling in Gravity and Magnetic Interpretation.* - Geophysics *43*, 912-929.

BOSUM, W. (1968): *Ein automatisches Verfahren zur Interpretation magnetischer Anomalien nach der Methode der kleinsten Quadrate.* - Geophys. Prospect. *16*, 107-126.

BRÜCKMANN, W. (1930): *Erdmagnetische Vermessung der Schweiz. I. Allgemeines, Deklination.* - Ann. schweiz. meteorol. Zentralanst. *7.*

— (1931): *Erdmagnetische Vermessung der Schweiz. II: Horizontalintensität, Inklination.* - Ann. schweiz. meteorol. Zentralanst. *6.*

CORSON, D.R., & LORRAIN, P. (1962): *Introduction to Electromagnetic Fields and Waves.* - Freemann & Co., San Francisco.

FISCHER, G., & SCHNEGG, P.-A. (1977): *Le Nouveau Levé Géomagnétique de la Suisse.* - Vermess., Photogramm., Kulturtech. *8*, 253-261.

FISCHER, G., SCHNEGG, P.-A., & SESIANO, J. (1979): *A New Geomagnetic Survey of Switzerland.* - Contr. Geol. Switzerl. [Geophys. Ser.] Publ. *19.*

GERARD, A., & DEBEGLIA, N. (1975): *Automatic Three-Dimensional Modeling for the Interpretation of Gravity or Magnetic Anomalies.* - Geophysics *40*, 1014-1034.

HJELT, S.-E. (1972): *Magnetostatic Anomalies of Dipping Prisms.* - Geoexploration *10*, 239-254.

JAMES, F. (1972): *Function Minimization.* - CERN Rep. *72/21.*

JAMES, F., & ROOS, M. (1975): *MINUIT - A System for Function Minimization and Analysis of the Parameter Errors and Correlations.* - Computer Phys. Comm. *10*, 343-367.

MCGRATH, P.H., & HOOD, P.J. (1970):*The Dipping Dike Case: a Computer Curve-Matching Method of Magnetic Interpretation.* - Geophysics *35*, 831-848.

— (1973): *An Automatic Least-Squares Multimodel Method for Magnetic Interpretation.* - Geophysics *38*, 349-358.

MERCANTON, P.-L., & WANNER, E. (1043): *Die Magnetische Anomalie im Jorat (Kanton Waadt). 1. Teil: Die Verteilung der Vertikalintensität.* - Ann. schweiz. meteorol. Zentralanst., Addendum.

— (1946): *Die Magnetische Anomalie im Jorat, Kanton Waadt. 2. Teil: Horizontalintensität und Deklination.* - Ann. schweiz. meteorol. Zentralanst. *6.*

MEYER DE STADELHOFEN, C., SIGRIST, W., & DONZÉ, A. (1973): *L'Anomalie Magnétique du Jorat.* - Bull. Lab. Géol. etc. Mus. géol. Univ. Lausanne *202.*

PLOUFF, D. (1976): *Gravity and Magnetic Fields of Polygonal Prisms and Application to Magnetic Terrain Corrections.* - Geophysics *41*, 727-741.

TALWANI, M. (1965): *Computation with the Help of a Digital Computer of Magnetic Anomalies Caused by Bodies of Arbitrary Shape.* - Geophysics *30*, 797-817.

WHITEHILL, D.E. (1973): *Automated Interpretation of Magnetic Anomalies Using the Vertical Prism Model.* - Geophysics *38*, 1070-1087.